



# Evaluation of geometrical defects in AWJM process of a hybrid CFRT/Steel structure

Fermin Bañón<sup>a,\*</sup>, Alejandro Sambruno<sup>a</sup>, Moises Batista<sup>a</sup>, Bartolome Simonet<sup>b</sup>, Jorge Salguero<sup>a</sup>

<sup>a</sup> School of Engineering, Mechanical Engineering and Industrial Design Department, University of Cadiz, Av. Universidad de Cadiz 10, Puerto Real, Cadiz E-11519, Spain

<sup>b</sup> Nanotures SL, C. Inteligencia 19, Tecnoparque Agroalimentario, Jerez de la Frontera, Cadiz E-11591, Spain

## ARTICLE INFO

### Keywords:

Geometrical defect  
Taper angle  
AWJM  
Machining  
Hybrid structure

## ABSTRACT

The bonding of Carbon Fibre Reinforced ThermoPlastic composites (CFRTP) and steel is of great interest nowadays. Nevertheless, the difference in machinability between dissimilar materials requires a specific machining process. Abrasive water jet machining is a flexible and environmentally friendly technology that can machine dissimilar materials at the same time with good results. However, due to the characteristics of the process and materials, geometrical defects such as taper angle can be caused by the loss of kinetic energy.

In this research, the study of the final geometry in abrasive waterjet machining of a hybrid CFRTP/Steel structure. A new methodology for the evaluation of taper angle with high accuracy has been developed through image processing. In addition, the surface quality in terms of  $R_a$  and  $R_z$  has been assessed. A potential-type trend between taper and hydraulic pressure has been established for both materials. Minimum taper values between 1.5° and 5° have been obtained for both materials and stacking configurations with a combination of a hydraulic pressure of 420 MPa, an abrasive mass flow of 225 g/min and a traverse speed of 50 mm/min.

## 1. Introduction

### 1.1. Introduction to abrasive water jet machining of dissimilar materials

Nowadays, the industry demands the use of new materials that improve the properties of the existing ones. An interesting type of material is the Carbon fibre Reinforced ThermoPlastic polymer matrix composites, CFRTP. These materials, like thermoset composites (CFRP, Carbon fibre Reinforced Polymers), achieve an excellent mechanical properties/weight ratio [1,2]. These characteristics are discussed by J. Jiao *et al.* and highlight their ability to be bonded to other dissimilar materials by laser bonding [1]. On the other hand, S. Berger *et al.* highlights the properties of these composite materials as a key aspect in the automotive sector and weight reduction [2]. In addition, CFRTPs provide high resistance to compression and high recycling efficiency compared to thermosets [3].

Due to these characteristics and the fact that the manufacturing times of these materials are shorter than thermosets, they are considered as strategic materials for sectors such as the automotive industry [4]. Also, due to their lightness, they are ideal for sectors such as the aeronautical or maritime industry due to the reduction in costs, in terms of energy

consumption [5,6].

In addition, there is a great interest in joining composite materials with metallic alloys in order to obtain hybrid structures of dissimilar materials [7–10]. J. Jiao *et al.* [7] focus on the optimization of the laser thermal bonding of a CFRTP/steel hybrid structure. R. Pahuja *et al.* [8] focuses on the machining of a CFRP/Ti stack by non-conventional technologies while A. Mahdi *et al.* [9] and J. Xu *et al.* [10] focus on the drilling of such structures. This type of structures can achieve mechanical properties that would not be obtained by each material separately. Furthermore, in terms of production, the manufacture and subsequent machining of both materials at the same time means a reduction in operating times [11]. The characteristics of thermoplastic composites to be able to reshape their geometry is a great advantage for obtaining hybrid structures. This allows a complete thermal bonding between both materials. This makes it easy to eliminate or minimize the use of mechanical rivet-type joints, reducing the final weight of the structure and improving its environmental impact [12]. At the same time, as there is a continuous union in the interlayer, it is not necessary to separate the materials after machining to evaluate the internal state of the interlayer, thus reducing the final costs.

Also, there is a current challenge in the sustainable and efficient

\* Corresponding author.

E-mail addresses: [fermin.banon@uca.es](mailto:fermin.banon@uca.es) (F. Bañón), [alejandro.sambruno@uca.es](mailto:alejandro.sambruno@uca.es) (A. Sambruno), [moises.batista@uca.es](mailto:moises.batista@uca.es) (M. Batista), [bartolome.simonet@nanotures.com](mailto:bartolome.simonet@nanotures.com) (B. Simonet), [jorge.salguero@uca.es](mailto:jorge.salguero@uca.es) (J. Salguero).

<https://doi.org/10.1016/j.ijmecsci.2021.106748>

Received 1 June 2021; Received in revised form 30 July 2021; Accepted 14 August 2021

Available online 18 August 2021

0020-7403/© 2021 The Author(s). Published by Elsevier Ltd. This is an open access article under the CC BY license (<http://creativecommons.org/licenses/by/4.0/>).

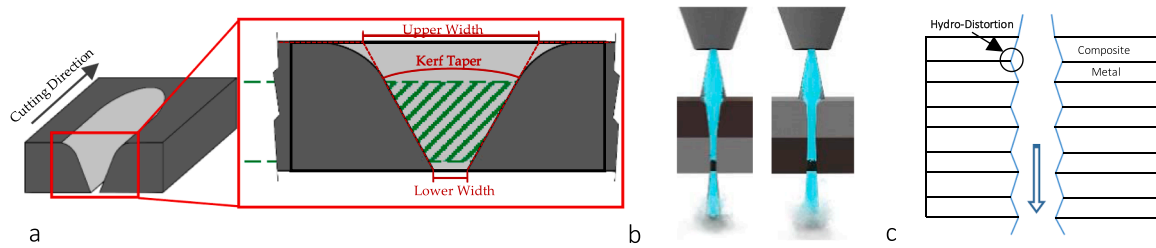


**Fig. 1.** Different geometrical defects after abrasive waterjet machining. a) Taper defect and width ratio; b) Taper geometry according to stacking order; c) Hydrodistortion defect due to the difference in machinability.

machining of hybrid structures made of dissimilar materials at the same time. Conventional machining technologies such as milling or drilling require Metalworking Fluids (MWF) to reduce the high temperatures that are reached due to shear and friction in the interface of the cutting edges with the materials [13–15]. J. Dionne *et al.* [15] Benefits of CO<sub>2</sub> Cooling as a cooling technology for drilling of stackup composite structures discusses the comparison between lubricants using MQL techniques and cryogenic cooling techniques as strategies to optimise conventional machining and reduce tool wear. However, the use of this type of lubricant is being eliminated or prohibited due to its high environmental impact [16], being also banned because of their negative connotations in terms of health, costs and environmental impact [17]. Thus, the use of cutting fluids can achieve a 17% of the final cost in the manufacturing of a product [18].

Because of this, initiatives such as CleanSky have been created. This project seeks the sustainable green machining, by minimizing the environmental impact and maximizing the efficiency of the machining process. This fact can reduce CO<sub>2</sub> emissions through lightweight structures, improving its performance [19].

On the other hand, due to the abrasive nature of the composite material and the low machinability of some kind of metals, the wear generated in the cutting tools requires the manufacture of very specific cutting-tool geometries, suitable for the machining of different materials at the same time, increasing the final cost of the process [11,13,20]. S. Fernández-Vidal *et al.* [11] discusses the main wear mechanisms (abrasion and adhesion) in dry drilling of a CFRP/UNS A97075 stack. Both types of wear reduce the effect produced by the other, resulting in lighter wear compared to the drilling of both materials separately. E. Adesta *et al.* [13] highlights the importance of a correct machining strategy in conventional operations such as milling in order to minimise cutting edge wear. X. Wang *et al.* [20] indicate in their research on drilling of hybrid structures that the overall tool wear is the combination of the edge rounding wear from drilling the top CFRP layer and the flank wear from drilling the bottom Ti layer without considering the edge chipping

The different machinability of each material requires a combination of different cutting parameters. Because of this, machining strategies arise that require changes of cutting parameters on the face of the machine. This change increases operating times and may affect the quality of the interface. In relation to machining temperatures, CFRTPs have thermal defects due to their low melting temperature. This can be easily overcome with conventional machining technologies. This allows the matrix to be removed and leads to poor surface quality and fibre pull-out defects. [21,22]. These conclusions are observed both in drilling operations performed in the research of A. Erturk *et al.* [21] and in milling operations of thermoplastic composites performed by P. Masek *et al.* [22].

An interesting green technology that can overcome the previous challenges is Abrasive Water Jet Machining (AWJM). From an environmental point of view, this process has high efficiency by using water at high pressure, that can be reused later reducing its negative impact on the environment. Compared to conventional technologies, there are no physical tools. Therefore, the wear and tear of auxiliary elements is

much lower, reducing process costs. [23]. In addition, N. Vu *et al.* [24] have studied the influence of nozzle diameter on abrasive blasting techniques in order to optimise the process and reduce costs.

In addition, this technology offers advantages such as the recovery of abrasive particles after machining, which can be reused after treatment, and no harmful gases are generated [25]. Another advantage is the reduction of cutting forces and temperatures, minimizing thermal defects in both materials -especially in CFRTPs- achieving a cleaner and more homogeneous cut [26,27].

Nevertheless, the machining of more than one material at the same time is an aspect that is currently being widely studied. Due to the difference in mechanical properties, each material has a different behaviour when interacting with the water jet, which generates a wide defectology that have to be studied and optimized.

This article proposes a study of abrasive waterjet machining in a hybrid CFRTP/Steel structure in its two stacking configurations. The cutting geometry has been evaluated using an image processing methodology, while surface quality has been evaluated in terms of  $R_a$  and  $R_z$ . Both aspects have been related to the cutting parameters by means of an experimental design, in order to study their influence through ANOVA statistical analysis. Finally, predictive mathematical models for kerf taper values have been obtained, while the main defects in the machining of both materials have been identified.

## 1.2. Literature review on abrasive waterjet machining of dissimilar materials

An inherent defect in waterjet machining is the formation of a conical geometry or taper angle, due to the loss of kinetic energy of the jet particles as they penetrate the material, reducing their cutting capacity, and resulting in a tapered cut (Fig. 1.a) [28,29]. In both investigations, M. Li *et al.* shows this loss of kinetic energy that generates a conical variation in geometry in the machining of a CFRP/Ti6Al4V hybrid structure and in the machining of a thick thermoset composite material. In addition, this defect is usually complemented with the erosive effect of the particles as they impact the top surface of the material, generating rounding edges that increases the conicity [30].

The stacking order of the materials that compose the hybrid structure also generates a new input variable that can affect the final quality [8, 31]. When the waterjet impacts on the material with the highest machinability, the reduction of kinetic energy is lower, generating a more homogeneous machining and geometry [32]. On the contrary, when the first material presents a worse machinability the waterjet reduces its cutting capacity by machining this material. This, together with the turbulence generated in the interlayer, produces a difference in cutting geometry and a greater conicity. In this sense, Ruiz-Garcia *et al.* [33] carried out a parametric study to evaluate the influence of cutting parameters and stacking order on abrasive waterjet cutting in an hybrid CFRP/UNS A92024 (Al-Cu) structure. The established variables were hydraulic pressure (120–250) MPa, feed speed (15–45) mm/min and abrasive mass flow (170–340) g/min. Their results indicate that the most suitable stacking order should be first the composite material followed by the metal alloy (lower to higher machinability). With this

**Table 1**  
Main characteristics of the thermoplastic composite material.

Final Thickness	Thermoplastic	Ply Orientation	Number of Plies	Fibre / Matrix (%)
2.1 mm	TPU (Polyurethane)	[0°/90°] <sub>s</sub>	7	74.2 / 25.8

sequence, most combinations of cutting parameters offer little variation in the conicity obtained in both materials, due to the fact that the waterjet suffers less loss of kinetic energy when passing through them.

Hourglass geometries (Fig. 1.b) are obtained when the metal alloy is the first material to be machined due to the turbulence generated in the interlayer that produces a divergence in the waterjet [34]. In parallel, when the hybrid structure is composed of multilayers of dissimilar materials (Fig. 1.c) a defect known as "hydrodistortion" arises. This is produced by the convergence and subsequent divergence of the water jet when machining both types of materials. The different mechanical properties and the loss of kinetic energy result in transverse machining at the interface [35,36]. R. Pahuja *et al.* [36] shows this defect in abrasive water jet machining of a graphite-titanium FML. The different properties of each thin layer allow the waterjet to machine transversely. This results in a geometrically varying profile. On the other hand, M. Rajesh *et al.* [35] indicate that this defect is directly related to hydraulic pressure. Low levels of this parameter produce a more irregular cut between dissimilar materials.

The metal alloy absorbs a higher amount of cutting energy, causing the jet to transversely machine the composite material and weakening the joints between the two materials, leading to separation in the interlayer or the formation of delaminations.

As is expected, the stacking sequence is also critical for surface quality. If the first material is the metal alloy, it absorbs most of the kinetic energy of the waterjet reducing its cutting capacity [37]. This produces a greater roughness in the composite material due to the plastic deformation impacts of the particles that eliminate the polymer matrix as it is the weakest element [38,39]. However, as the jet does not have enough energy, it bends the reinforcement without eliminating it completely, generating fibre pull-out defects [28]. Thus, the most relevant factor in the surface quality seems to be the traverse speed as indicated by Alberdi *et al.* [40]. A greater stabilization of the waterjet will be obtained at controlled traverse speed, ensuring a constant flow of particles.

On the other hand, the erosive effect can distort the taper evaluation obtained in the machining of hybrid structures applying the traditional methodology, which is generating new studies focused on developing more accurate evaluation methodologies [41]. As indicated by Li *et al.* [28] the kerf profile can present a curvature due to the effect of the erosive particles generating a great deviation between the kerf profile and the union by means of a linear regression that joins the points that define the upper and lower width after the machining. Thus, the formation of this taper in both materials is strongly influenced by the hydraulic pressure of the water jet [42]. This generates a higher energy to the waterjet capable of machining both materials at the same time. However, this cutting capacity can be preserved by increasing the abrasive mass flow, reducing the conicity obtained. In the same way, better results are obtained by reducing the dispersion of the kinetic energy of the waterjet [43]. When the material thickness is very high, it is recommended to increase the hydraulic pressure and reduce the traverse speed. This reduces the dispersion of the kinetic energy of the waterjet during machining by minimizing the conicity [44,45]. On the contrary, the increase in the traverse speed and the reduction of pressure generate an unstable and turbulent flow, generating a rougher surface and the formation of grooves or lakes at the outlet of the waterjet [33].

Based on the scientific literature, there seems to be a general consensus on the influence of traverse speed and hydraulic pressure on the reduction of taper angle and the improvement on surface quality

[42,44,46–48]. K. Manoj *et al.* [42] studies the taper generated in the machining of fibre-reinforced composites. They report that there is a direct relationship between hydraulic pressure and traverse speed with the top width obtained and the final taper. H. Youssef *et al.* [44] also focus on the machining of composite materials by this technology. They indicate that an increase in this parameter reduces both the upper and lower width of the cut. In order to reduce the taper generated by high traverse speed, P. Karmiris-Obratanski *et al.* [48] carry out research on multi-passes to improve the efficiency of the process. The literature review on this subject by R. Thakur *et al.* [46] indicates that the taper defect is related to energy loss. To optimise the taper defect and reduce energy loss, low levels of traverse speed are necessary.

In addition, the literature indicates the importance of the stacking order and it is recommended to place the metal alloy as a second material to minimize the dispersion of kinetic energy of the waterjet. This is in line with the previously mentioned, the difference in machinability between the materials of the hybrid structure is one of the most relevant aspects in water-jet machining. H. Youssef *et al.* [44] also focus on the machining of composite materials by this technology. They indicate that an increase in this parameter reduces both the upper and lower width of the cut.

Most of the previous literature is focused on hybrid structures that are made up of thermosetting composite materials and light metallic alloys, that are joined together mechanically as is usual in aeronautics. The use of mechanical joints can form a gap between materials, increasing the turbulence in the interlayer and enhancing the taper defect. In turn, this type of union requires a subsequent separation of the materials to verify the state of the interlayer.

In this sense, thermal or adhesive joints can be a very interesting alternative, in order to minimise defects in the interlayer and reduce production times. This fact could be of relevance in the machining of hybrid structures on thermoplastic composites and steel alloys, that can be easily joined by thermal or adhesive processes [49–51]. Nevertheless, there is a lack of researches about this field in the scientific literature. Thus, the stacking sequence must be studied in order to determine the final state of the interface and to ensure a constant geometry in both materials. Moreover, traditional methodologies for evaluating conicity does not take into account the erosive effect of abrasive particles.

## 2. Experimental methodology

Materials, equipment and machining strategies will be explained in the following sections. The materials that compose the hybrid structure, as well as their fabrication process will be explained in this section indicating the surface preparation process of the metal alloy. Subsequently, the selected machining technology as well as the experimental design will be shown. The aim is to set the influence of the cutting parameters on the final geometrical quality for both stacking configurations.

Finally, a new methodology for the correct evaluation of the taper defect after water jet machining is proposed as a novelty. This methodology is based on the image processing of the grooves to obtain the real profile and separate the taper defect from the erosion defect. In addition, the surface quality has been evaluated and predictive mathematical models have been developed.

### 2.1. Materials and equipment

For the development of this research two dissimilar materials have been joined in order to obtain a hybrid structure. On the one hand, a thermoplastic composite material reinforced with carbon fibre (Twill 200 gr/m<sup>2</sup>) has been used. The thermoplastic matrix is polyurethane and its main characteristics and mechanical properties are shown in the Table 1. The composite material has been obtained by thermoforming.

On the other hand, a carbon steel S275 with a thickness of 3 mm has been used as the second material of the hybrid structure. This is a

**Table 2**

Composition (% mass) and main mechanical properties of S275 carbon steel.

%C	%Fe	%Mn	%P	%S	%Si
0.25	98.01	1.60	0.04	0.05	0.05
Yield Strength (MPa)			Tensile Strength (MPa)		
275			450		

**Table 3**

Cutting parameters for abrasive waterjet texturing.

Hydraulic Pressure-P (MPa)	Abrasive Mass Flow-AMF (g/min)	Traverse Speed-TS (mm/min)
250–340–420	225–340–385	50–100–300

structural steel of great interest in various industrial applications due to its mechanical properties and its current interest in bonding with composite materials [52]. The main characteristics of this steel are shown in the Table 2.

The steel surface has been modified by shot blasting with a pressure of 0.5 MPa, corundum particles of size 630  $\mu\text{m}$  and an impact distance of 100 mm in order to increase the surface free energy and obtain a quality

bond between the two materials [53]. These materials were joined by means of a hot plate press. This allows the change from solid to liquid state of the thermoplastic matrix, filling the rough surface of the steel alloy. Finally, after a subsequent cooling, the matrix consolidates again generating a continuous bond between both materials.

For the trials, a Waterjet Machine (TCI Cutting, BP-C 3020, Valencia, Spain) has been used. The nozzle of the machine has a diameter of 0.8 mm, an orifice diameter of 0.3 mm and a nozzle length of 94.7 mm. The AWJM machine is equipped with an ultra-high capacity pump (KMT, 158 Streamline PRO-2 60, Bad Nauheim, Germany). All trials were carried out by a 120 mesh Indian Garnet abrasive particles.

Three cutting parameters have been modified based on the literature consulted: Hydraulic Pressure ( $P$ ), Abrasive Mass Flow ( $AMF$ ) and Traverse Speed ( $TS$ ). The stand-off distance has been set at 3 mm, and three levels per cutting parameter have been applied obtaining a total of twenty-seven combinations of cutting parameters (Table 3). In order to obtain greater repeatability and robustness, each combination has been repeated twice.

In addition, the stacking sequence has been also studied. The experimental design has been made for the CFRTP/Steel configuration and the reverse, Steel/CFRTP.

In order to ensure a constant flow of abrasive and water, together

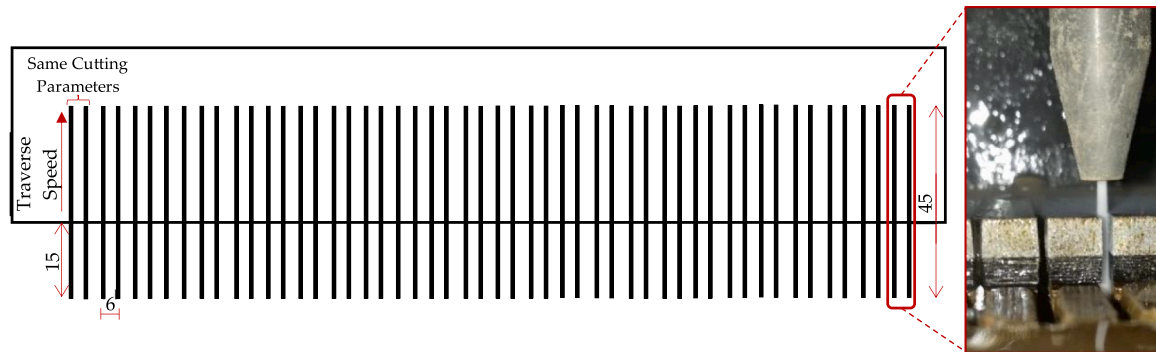


**Fig. 2.** Graphic representation of the established experimental design. All tests start 15 mm from the edge of the material to obtain a stable flow of water and abrasive. Each combination of cutting parameters has been repeated twice.

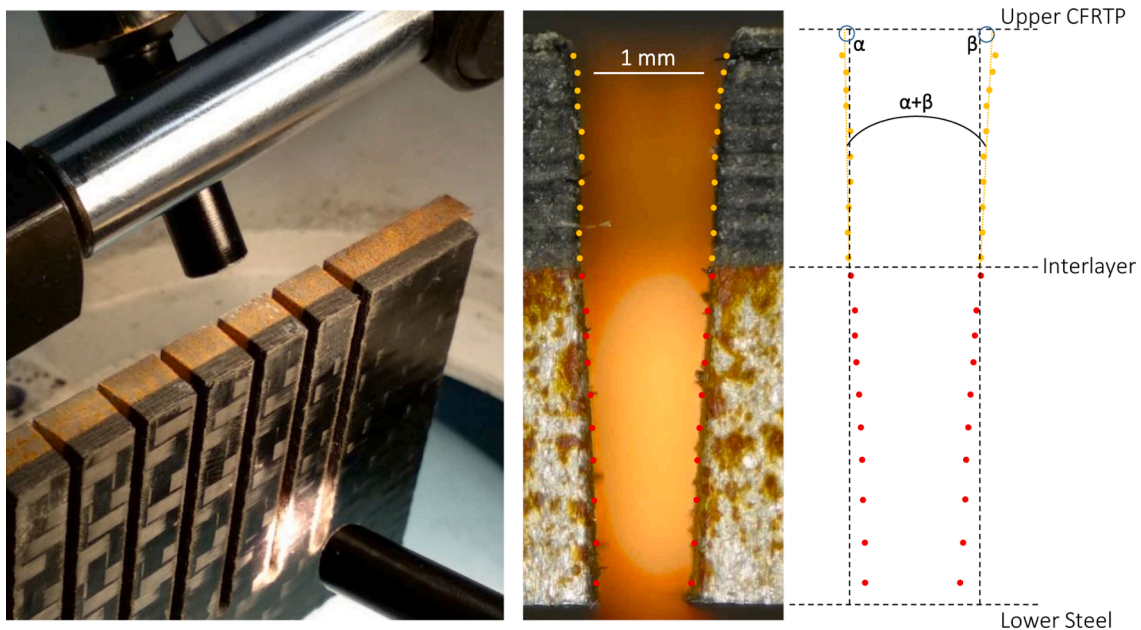


**Fig. 3.** Proposed methodology for the correct measurement of the taper defect. Using a set of lights and image processing software, the coordinates of 10 points per material and side are obtained. Linear approximations to these points allow to obtain the taper in angular terms.



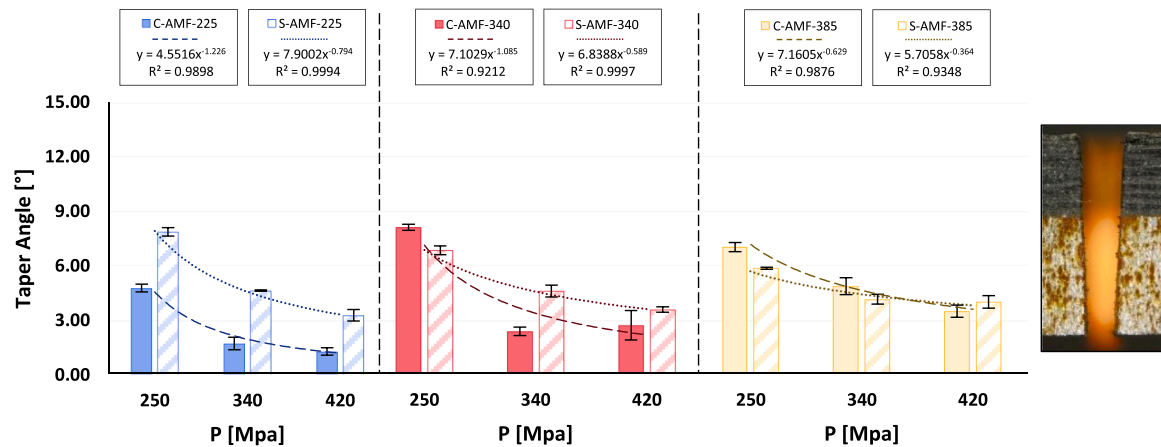


Fig. 4. Taper angles as a function of hydraulic pressure (P: 250–420 MPa) and abrasive mass flow (AMF: 225–385 g/min) for CFRT/Steel stack configuration.

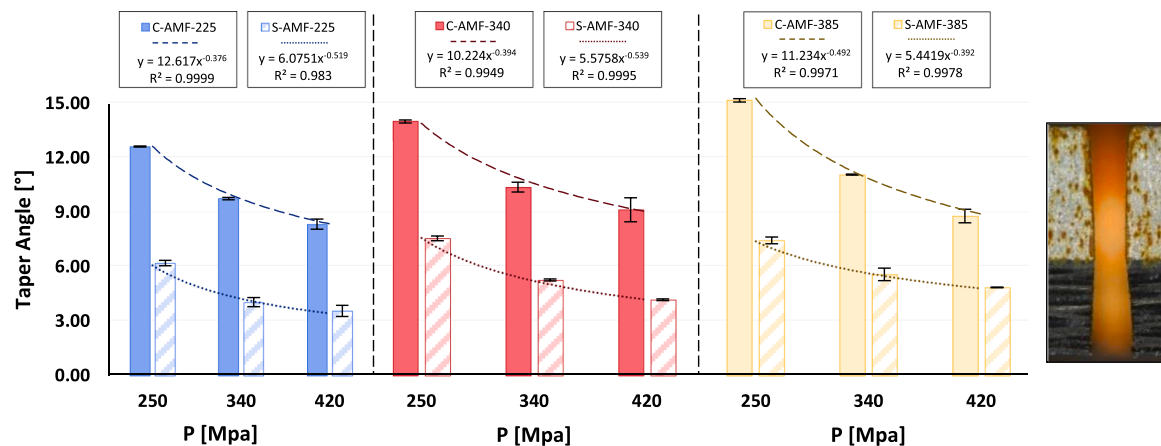


Fig. 5. Taper angles as a function of hydraulic pressure (P: 250–420 MPa) and abrasive mass flow (AMF: 225–385 g/min) for Steel/CFRT stack configuration.

with a constant traverse speed, each test starts with a 15 mm gap to the hybrid structure, as is shown in Fig. 2.

## 2.2. Evaluation methodology

The traditional methodology for evaluating the taper generated in water-jet machining is to establish a relationship between the upper and lower widths. Nevertheless, the current scientific literature reports that this type of methodology can distort the results. This is due to an interaction between the generated taper and the erosion generated by the abrasive particles at the beginning of the cut [54].

Due to this, an alternative methodology based on image processing is proposed (Fig. 3). Thus, a stereoscopic microscope (Nikon, SMZ 800, Tokyo, Japan) has been used to make macrographs perpendicular to the slots obtained. A supplementary cold light source has been used in order to illuminate inside of the slot for obtaining a defined machining profile.

For each macrograph, an image processing software (ImageJ, National Institutes of Health) has been used to determine the profile coordinates of each side of the cut. With this point cloud, a linear regression has been carried out on these points, detecting the intersection of this line with the upper and lower widths. Knowing the gradient and cut in order of each regression, the taper angle of the left ( $\alpha$ ) and right ( $\beta$ ) sides can be calculated. In this investigation, the sum of both angles has been considered as the final taper angle ( $\alpha + \beta$ ), Fig. 3.

Surface quality has been evaluated in terms of  $R_a$  and  $R_z$  by using a roughness-metre (Mahr Perthometer PGK 120, Göttingen, Germany).  $R_a$  is the standard parameter for evaluating surface quality after machining. Nevertheless, in order to complement the information obtained by

means of this parameter,  $R_z$  provides more detailed information on the peak-to-valley distances generated in the roughness profile. Three measurements have been made for each material (CFRT and Steel) for each machining test and in both stacking configurations. The surface quality evaluation has been carried out following ISO 4288:1999 standard. A cut-off of 2.5 mm was established for a total evaluation length of 12.25 mm. Stylus with 2  $\mu$ m tip radius and 90° tip angle was used for the measurements, reference M-250 from Mahr.

Finally, defects related to the machining process such as delaminations, gaps in the interlayer or loss of matrix on the machined surface have been identified.

Furthermore, the influence of cutting parameters on the results obtained has been determined by means of an ANOVA statistical analysis (18.1, Minitab, LLC, State College, PA, USA). To conclude, a series of contour diagrams that relate these parameters to the results obtained have been obtained and the combination of parameters that minimise the conicity obtained and generate the best surface quality has been determined.

## 3. Results and discussions

The final geometrical quality after each machining test is presented in this section. The individual influence of each parameter selected in the experimental design has been studied with respect to the taper obtained. In turn, the results have been approximated to exponential trends with a high level of fit. In order to study the influence of materials, the results have been compared for the same combination of shear parameters in both stacking configurations. This allows to establish the

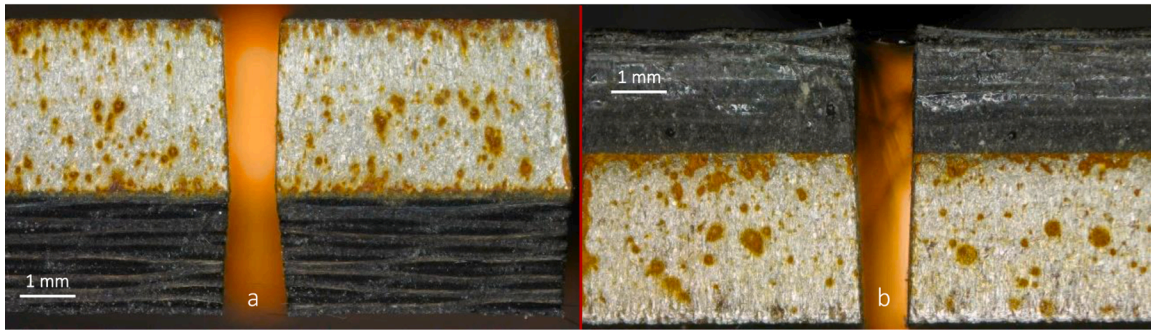


Fig. 6. Variation in conical geometry as a function of material stacking order for 420 MPa and 385 g/min for: a) Steel/CFRTP; b) CFRTP/Steel.

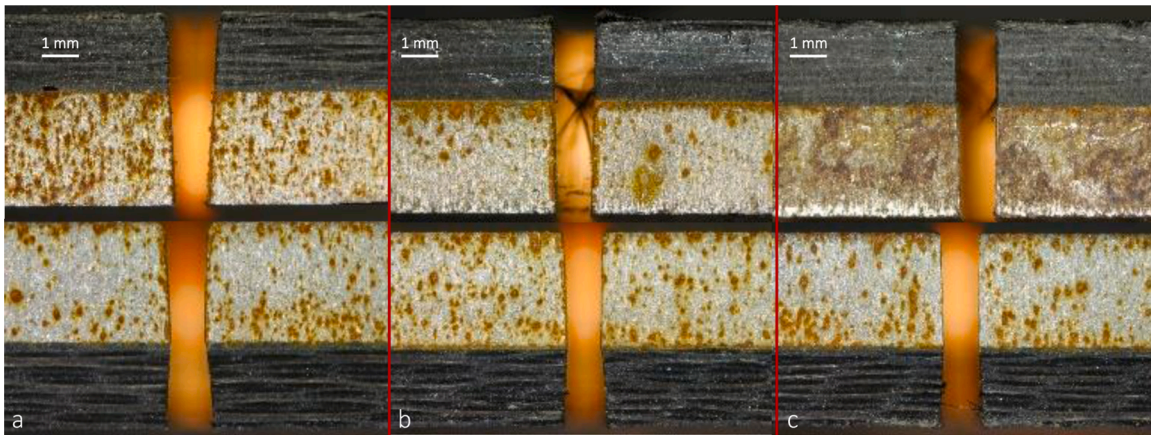


Fig. 7. Influence of hydraulic pressure on the conical defect for a TS of 50 mm/min, an AMF of 225 g/min: a) P 250 MPa; b) P 340 MPa; c) P 420 MPa.

dominant material in the hybrid structure for this machining process.

Finally, the relationship between the main cutting parameters and the final geometrical quality has been established through predictive models based on a response surface methodology. This has allowed to establish a statistical ANOVA analysis in order to determine the order of influence of the selected parameters and to establish an optimal combination for each stacking configuration.

### 3.1. Influence of hydraulic pressure and abrasive mass flow

An incorrect selection of cutting parameters in waterjet machining can result in very high conicity in the cutting profile of the hybrid structure. This can result in incorrect geometries causing elements to be rejected by quality controls after machining. The Fig. 4 shows the taper angle obtained by increasing the hydraulic pressure and abrasive mass flow for a fixed traverse speed of 100 mm/min for CFRTP/Steel stack. In this graph, "C" refers to composite material and "S" to steel.

As can be seen, the conicity obtained in both materials is greatly affected by the order of stacking in the hybrid structure. High taper angle values, close to  $13^\circ$ , are obtained when the first material to machine is steel, in comparison with reverse configuration. Thus, in the CFRTP/Steel configuration for a pressure of 250 MPa and an abrasive mass flow of 225 g/min, angles close to  $5^\circ$  are obtained for composite material and  $8^\circ$  for steel. In comparison, in the Steel/CFRTP configuration, values of  $13^\circ$  are obtained for the composite material and  $6^\circ$  for the steel alloy (Fig. 5).

As was mentioned before, this fact is due to the absorption of kinetic energy by the metal alloy, and is in agreement with Kumar *et al.* [55]. In this sense, the CFRTP/Steel configuration offers the lowest taper values in both materials, as well as very close results in both materials. Nevertheless, in the reverse configuration, a large part of the kinetic

energy is dispersed when machining the metal alloy, reducing its machining capacity. In addition, as indicated by Pahuja *et al.* [8], the waterjet changes from convergence to divergence in the hybrid structure interlayer, changing the orientation of the taper in the composite material due to the formation of turbulence. This variation is due to the stacking order of the materials and their different machinability. When machining steel first, a greater amount of kinetic energy is required to be cut. At the interface, the water jet produces a series of turbulences due to the different mechanical properties of the two materials. In this configuration, the composite material offers less resistance than steel. This causes that the water jet changes from a converging state to a diverging state.

This results in higher conicity values in all tests on the composite material for the CFRTP/Steel configuration. However, due to the different machinability of each material, visual defects such as delaminations are observed when the composite material is the first material machined. The layers that compose the composite material are separated at the beginning of the machining due to the erosive effect of the particles, producing a first separation in the form of delamination. On the contrary, when the composite material is the second material, the steel acts as a protective material, reducing the impact suffered by the composite material which prevents separation in the interlayer and the formation of delaminations (Fig. 6).

On the one hand, the influence of the hydraulic pressure on the taper obtained is the same for both configurations. An increase in this parameter increases the penetration capacity of the waterjet, reducing the resistance of both materials to be machined [56]. In addition, the results obtained can be adjusted to potential trends as indicated, with  $R^2$  values above 90%. Thus, small values of taper in water-jet machining require high values of hydraulic pressure as indicated by the results of Dhanawade *et al.* [57]. In this sense, the Fig. 5 shows the variation of

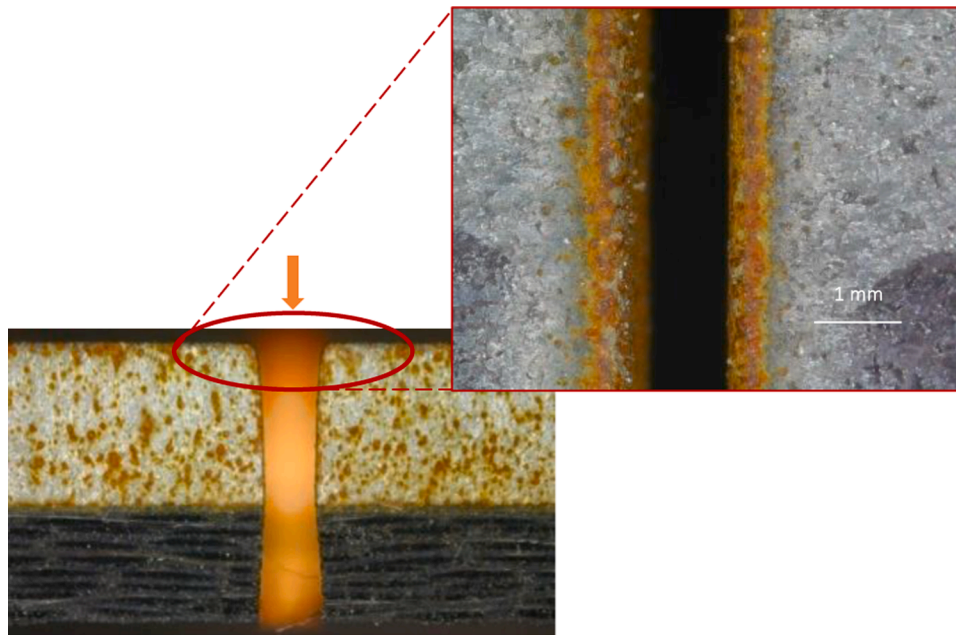


**Fig. 8.** Visual defects for a TS of 50 mm/min a P of 250 MPa and an AMF of 385 g/min. Rounding at the beginning of the machining due to the erosive effect and Area affected by erosion at the beginning of the machining.

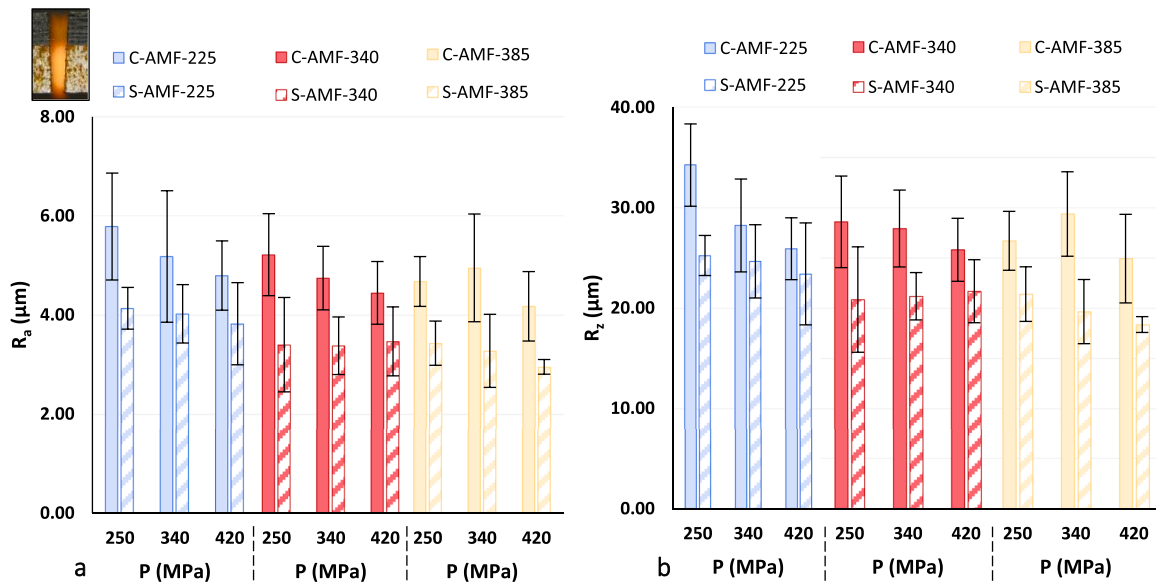


**Fig. 9.** Surface quality as a function of hydraulic pressure (P: 250–420 MPa) and abrasive mass flow (AMF: 225–385 g/min) for CFRT/Steel stack configuration: a)  $R_a$  Values; b)  $R_z$  Values.

taper in both materials for the two stacking configurations. An almost straight machining can be seen for both configurations when the hydraulic pressure is 420 MPa.

On the other hand, the effect of abrasive flow has a minor effect compared to hydraulic pressure. Nevertheless, especially in the steel alloy, the increase of this parameter reduces the taper obtained, although its influence is reduced by increasing the hydraulic pressure. The increase of the abrasive increases the penetration capacity of the waterjet in both materials (Fig. 7).

This leads to a lower resistance of the material to be machined, generating a lower dispersion in the kinetic energy of the jet and generating more homogeneous cuts. This is especially relevant when the configuration of the structure is Steel/CFRT as there is a greater variation of results between both materials.

Conversely, an excessive increase in abrasive mass flow increases the erosion of abrasive particles on the top surface of the material, especially on the steel alloy. Thus, the Fig. 8 shows the rounding effect in the steel when it is the first material and the abrasive mass flow is maximum. On the other hand, the figure shows the area affected by erosion along the whole cut (upper view). For this combination of cutting parameters, the machining capacity of the waterjet is minimal as the hydraulic pressure is the lowest value. On the other hand, the amount of abrasive particles is excessively high, producing intercollisions between them and reducing their cutting capacity. Finally, when combined with a speed of 50 mm/min, the amount of abrasive particles impacting during an instant of time is maximum, increasing the area affected by erosion [58].

Furthermore, surface quality values in terms of  $R_a$  and  $R_z$  for both stacking configurations are shown in Fig. 9 and Fig. 10. Trend lines have



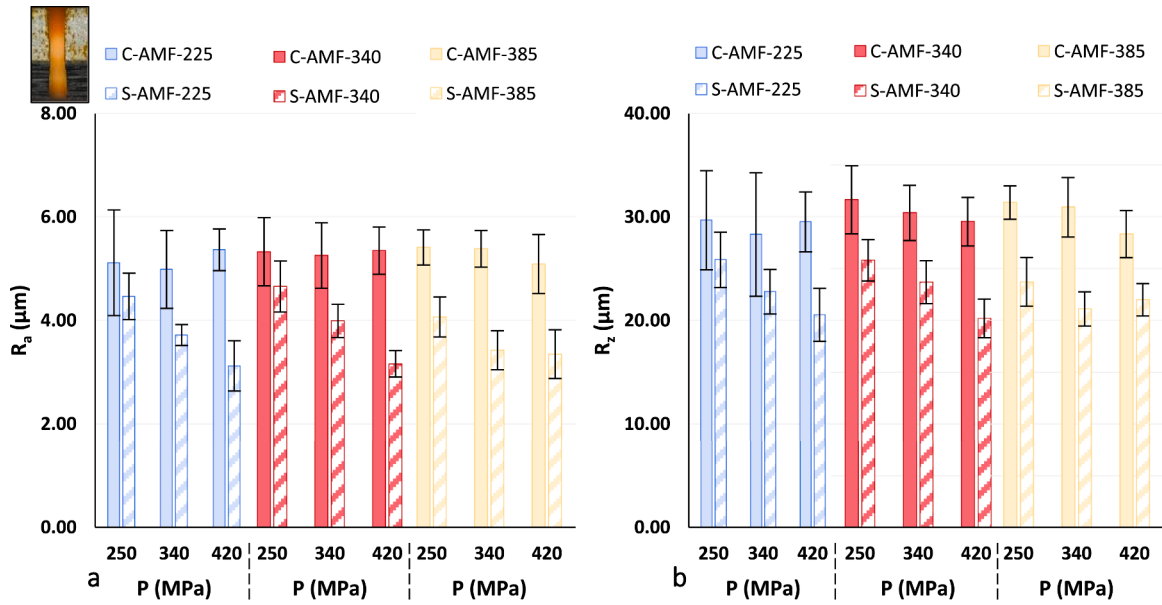


**Fig. 10.** Surface quality as a function of hydraulic pressure (P: 250–420 MPa) and abrasive mass flow (AMF: 225–385 g/min) for Steel/CFRTP stack configuration: a)  $R_a$  Values; b)  $R_z$  Values.



**Fig. 11.** Remains of the thermoplastic matrix adhering to the surface after machining that worsen surface quality.

not been represented because the adjustment obtained was not representative. This may be due to the anisotropic nature of the composite material and the heterogeneity of the hybrid structure.

In accordance with the results obtained by Pahuja *et al.* [34], higher  $R_a$  and  $R_z$  values are obtained in the composite material compared to steel. The anisotropic nature of these materials in combination with the aforementioned hydrodistortion defect produce a rougher surface with a greater distance between peaks and valleys [32]. In this sense, due to the

low cohesion between the thermoplastic matrix and the carbon fibre reinforcement, the shear stresses of the waterjet cause the matrix debris to detach and adhere to the machined surface (Fig. 11) worsening the surface quality results as explained in [59].

With regard to the stacking order, close values of surface quality are obtained in both cases in the composite material. Nevertheless, there seems to be a greater homogeneity of results for the Steel/CFRTP stack. In these case there does not seem to be an influence of the pressure on the surface quality. On the contrary, for the CFRTP/Steel stack, both parameters (pressure and abrasive) seem to reduce the quality obtained when increased. In accordance with the results of Ming *et al.* [60], this increase improves the cutting capacity of the waterjet, removing the material more easily and reducing the thermoplastic matrix residues on the surface which improves the  $R_a$  and  $R_z$  values.

On the other hand, decreasing trends are observed with the increase of hydraulic pressure and abrasive mass flow have been observed for steel values. As with the taper angle, the increase in hydraulic pressure and abrasive mass flow significantly increases the penetration capacity of the waterjet. The resistance to being eroded and machined in both materials is reduced and the machined surface presents a more homogeneous and less rough state. However, the influence of pressure is more remarkable in the Steel/CFRTP stack. For this configuration, the influence of the composite material and the kinetic energy loss due to the hydrodistortion defect is less. This increases the cutting ability of the waterjet on the steel. This allows to take advantage of the improvement

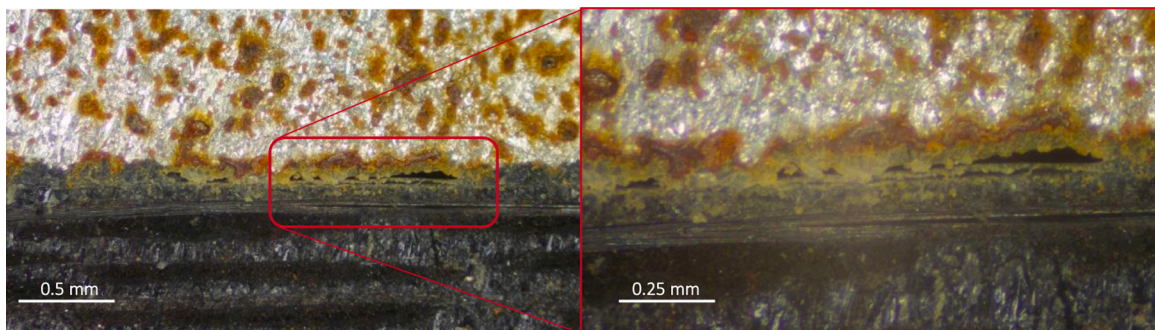


**Fig. 12.** Separation at the interface due to turbulent flow from a material with poorer machinability to a material with better machinability in the Steel/CFRTP configuration.



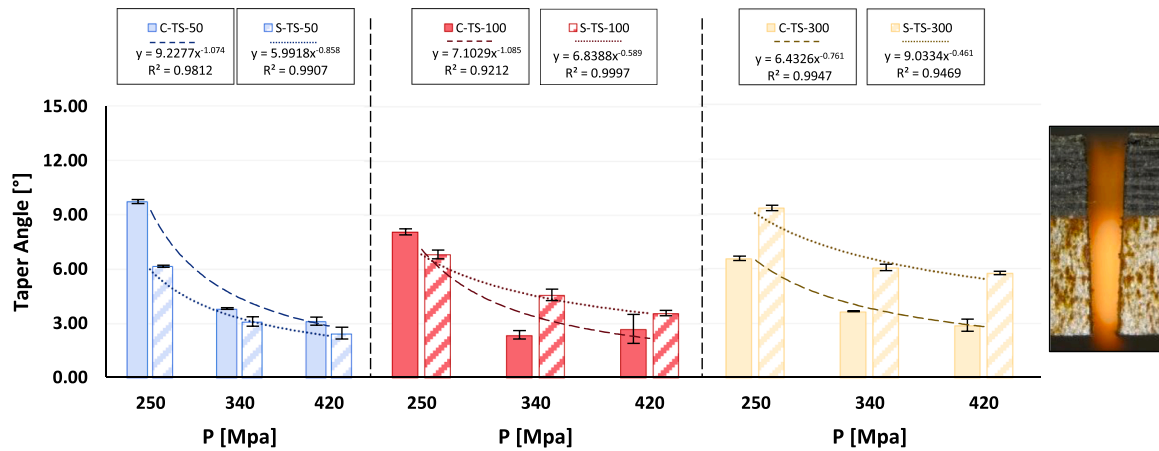


Fig. 13. Taper angles as a function of hydraulic pressure (P: 250–420 MPa) and traverse speed (TS: 50–300 mm/min) for CFRTP/Steel stack configuration.

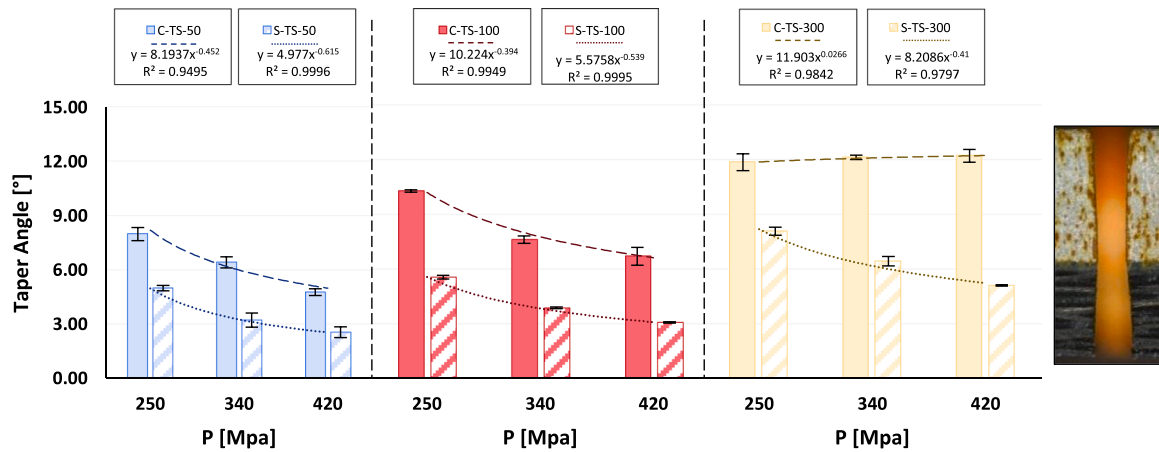


Fig. 14. Taper angles as a function of hydraulic pressure (P: 250–420 MPa) and traverse speed (TS: 50–300 mm/min) for Steel/CFRTP stack configuration.

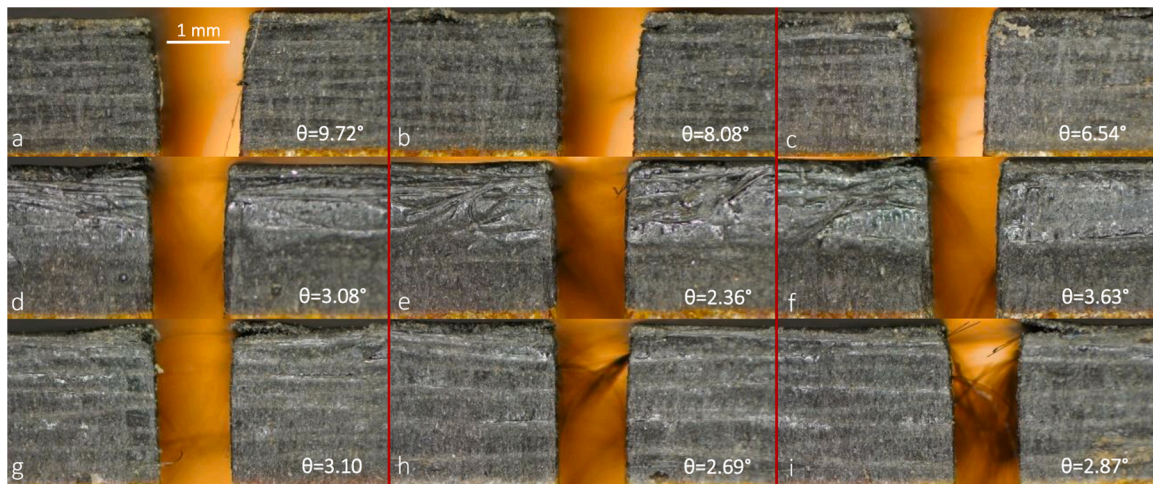
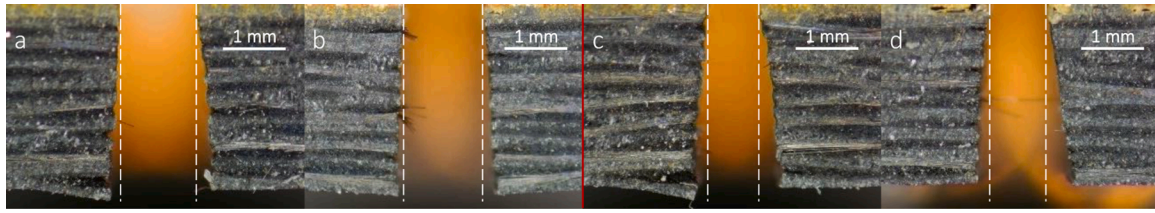


Fig. 15. Influence of the interaction between hydraulic pressure and traverse speed for a fixed abrasive flow rate (340 g/min): a) 250 MPa and 50 mm/min; b) 250 MPa and 100 mm/min; c) 250 MPa and 300 mm/min; d) 340 MPa and 50 mm/min; e) 340 MPa and 100 mm/min; f) 340 MPa and 300 mm/min; g) 420 MPa and 50 mm/min; h) 420 MPa and 100 mm/min; i) 420 MPa and 300 mm/min.

in kinetic energy by increasing the hydraulic pressure. In addition, a small gap in the interlayer has been detected for the combination of 340 MPa, 100 mm/min and 340 g/min (Fig. 12). This defect may have produced by the turbulence produced in the interlayer due to the conversion of convergence to divergence of the waterjet in combination

with the loss of penetration capacity when the steel has been machined. As in the case of hydrodistortion defects or the formation of delaminations in composite material [57], the flow of water in the interlayer may have eliminated the thermoplastic matrix that joins the two materials, producing this defect.



**Fig. 16.** Taper angle variation in Steel/CFRTP configuration for: a) P 250 MPa and TS 50 mm/min; b) P 420 MPa and TS 50 mm/min; c) P 250 MPa and TS 300 mm/min; d) P 420 MPa and TS 300 mm/min.

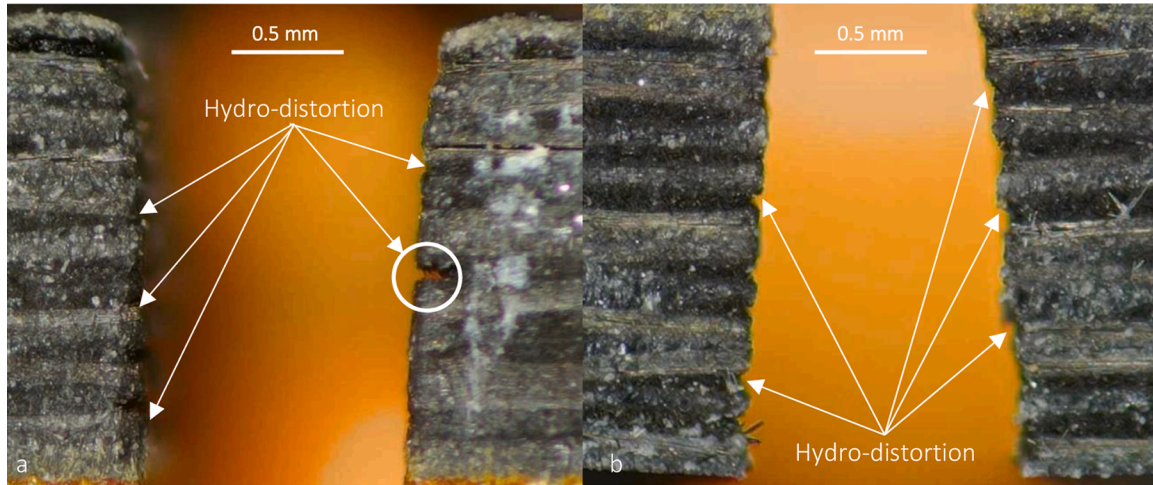


**Fig. 17.** Hydrodistortion defect generated due to the different machinability between the layers that constitute the composite material: a) CFRTP/Steel; b) Steel/CFRTP.

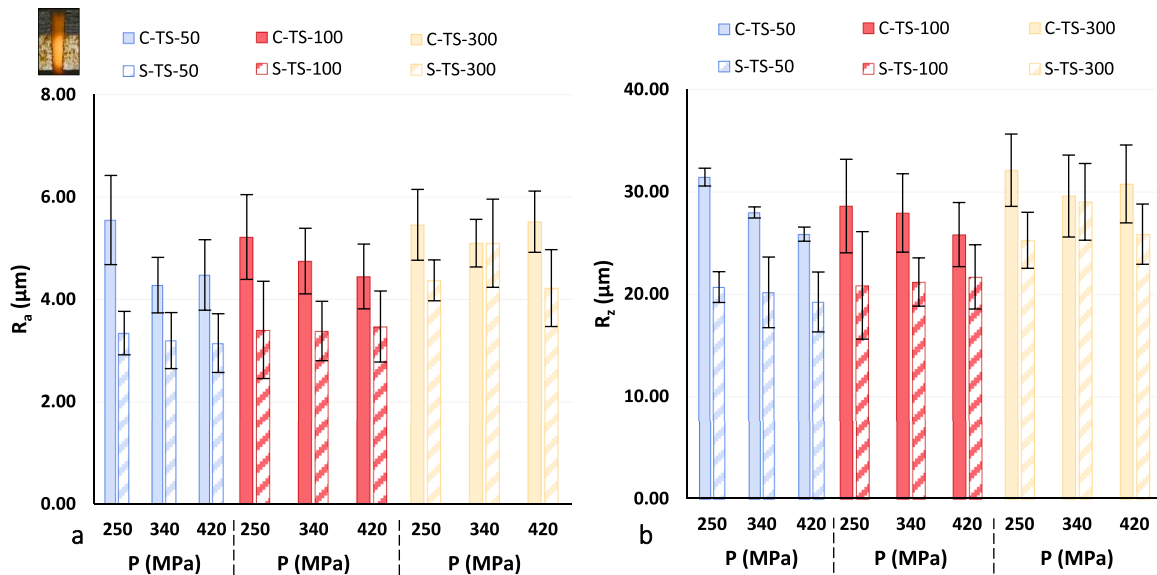


**Fig. 18.** Surface quality as a function of hydraulic pressure (P: 250–420 MPa) and traverse speed (TS: 50–300 mm/min) for CFRTP/Steel stack configuration: a)  $R_a$  Values; b)  $R_z$  Values.

### 3.2. Influence of hydraulic pressure and traverse speed

A combination of hydraulic pressure and waterjet traverse speed is essential to reduce the cutting conicity [33]. The taper angle values combining these parameters for a constant AMF of 340 g/min are shown in the Fig. 13 for CFRTP/Steel stack and Fig. 14 for Steel/CFRTP Stack.

As can be seen, the results obtained can also be approximated to a

potential trends with good fit (more than 94%). Minimum taper values are obtained with a hydraulic pressure of 420 MPa. Similarly, the highest taper values are obtained in the Steel/CFRTP configuration, especially at high traverse speeds (300 mm/min).

Along with the loss of kinetic energy when the jet machining the steel, the use of a high traverse speed produces an irregular and turbulent cut. In this sense, the amount of abrasive particles and water that

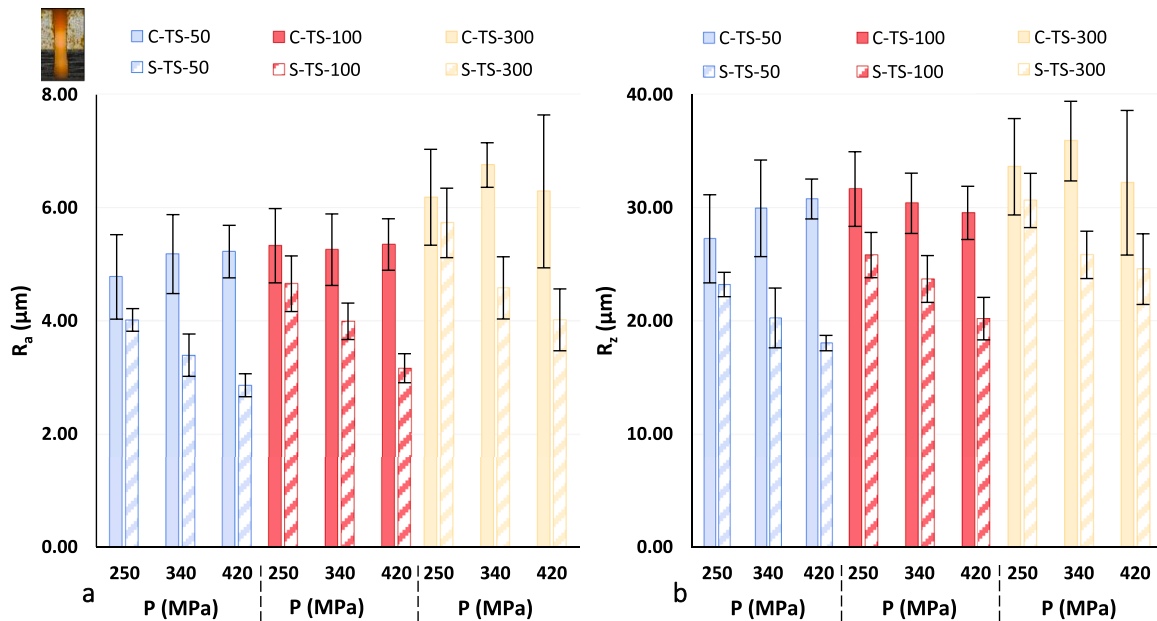


Fig. 19. Surface quality as a function of hydraulic pressure (P: 250–420 MPa) and traverse speed (TS: 50–300 mm/min) for Steel/CFRTP stack configuration: a)  $R_a$  Values; b)  $R_z$  Values.

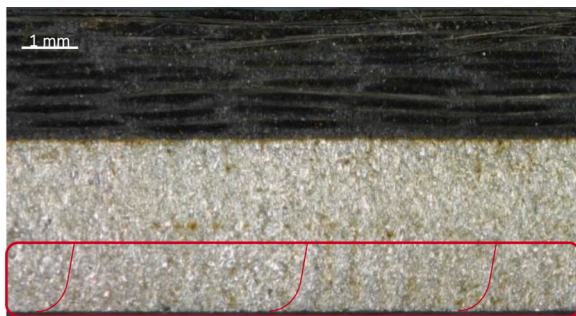


Fig. 20. RCR region due to lag defect caused by a high loss of kinetic energy that generates a greater destabilization of the water jet (340 MPa, 340 g/min and 300 mm/min).

machine the material is not homogeneous, producing that the jet is unstable and unable to machine the same amount of material. This fact produces taper angle differences of almost  $6^\circ$  in the composite material.

For the CFRTP/Steel configuration, the increase in traverse speed produces different trends in each material. The most direct is that observed in the steel alloy. The increase in this parameter, in combination with its greater difficulty to be machined, produces an increase in the taper angle in all three pressures used, being in agreement with similar results by [61]. On the other hand, in the composite material two trends are observed depending on the established pressure.

With a minimal pressure (250 MPa), a reduction of the taper is produced by increasing the traverse speed. This may be due to the erosive effect of the abrasive. If the traverse speed is very low, the low capacity of penetration of these particles can generate a great opening in the initial zone, provoked by the erosion generated until the stabilization of the machining. When the water jet passes through the composite material and converges due to the loss of kinetic energy, a taper is produced at the end of the thickness. Also, an increase in TS produces less interaction of the abrasive flow, generating a straighter cut in the composite material (Fig. 15).

On the contrary, by increasing the hydraulic pressure and minimizing the dispersion of the waterjet, the conicity obtained in the composite material undergoes a very small variation with results close to

$4^\circ$

Different trends are observed when the stacking is inverse, especially in the composite material. The taper generated in steel always increases with high traverse speeds. An increase in this parameter produces greater instability in the machining because it is not capable of machining the same amount of material in the same time interval. This causes a more turbulent flow that reduces its kinetic energy in the first moments of the machining, reducing the width of the final machining in the steel and increasing its conicity. In agreement with previous results and in the same line that was indicated by El-Hofy *et al.* [23], this trend is reduced with increasing hydraulic pressure. This increase allows a greater stabilization of the waterjet, increasing its penetration capacity and reducing the resistance of the material to be machined.

With regard to the composite material, only an increasing trend is observed for this configuration. The position of the steel as the first material acts as a shield, receiving the impact of the jet with its maximum penetration capacity. This fact reduces the impact received by the composite material and, together with the turbulent flow generated in the interlayer, increases the dispersion of the waterjet as it leaves the composite material. In the same way that the results obtained with steel, the pressure generates a decreasing potential trend due to the increase in the penetration capacity of the waterjet, with the exception of the application of a displacement speed of 300 mm/min [62]. For this level, the destabilisation of the jet is such that the hydraulic pressure levels are insufficient to correctly machine both materials, and producing taper values close to  $12^\circ$  for the three pressures applied (Fig. 16).

Finally, a typical defect generated in the machining of hybrid structures by waterjet with abrasive is the separation in the interlayer due to the different machinability of the materials, defect so-called as Hydrodistortion [36]. Hydrodistortion defects in the interlayer metal/composite have not been observed in the machined sections, however, the mechanism of this defect has been detected in the machined surface of the thermoplastic composite material, as is shown in Fig. 17.

This hydrodistortion is due the shear forces of the waterjet, that eliminate the thermoplastic matrix, allowing a transversal flow that generates small periodic cavities during the machining process. This can lead to the propagation of larger cracks in the form of internal delaminations.

The combination of traverse speed and hydraulic pressure also has a significant effect on surface quality. As with the combination of abrasive



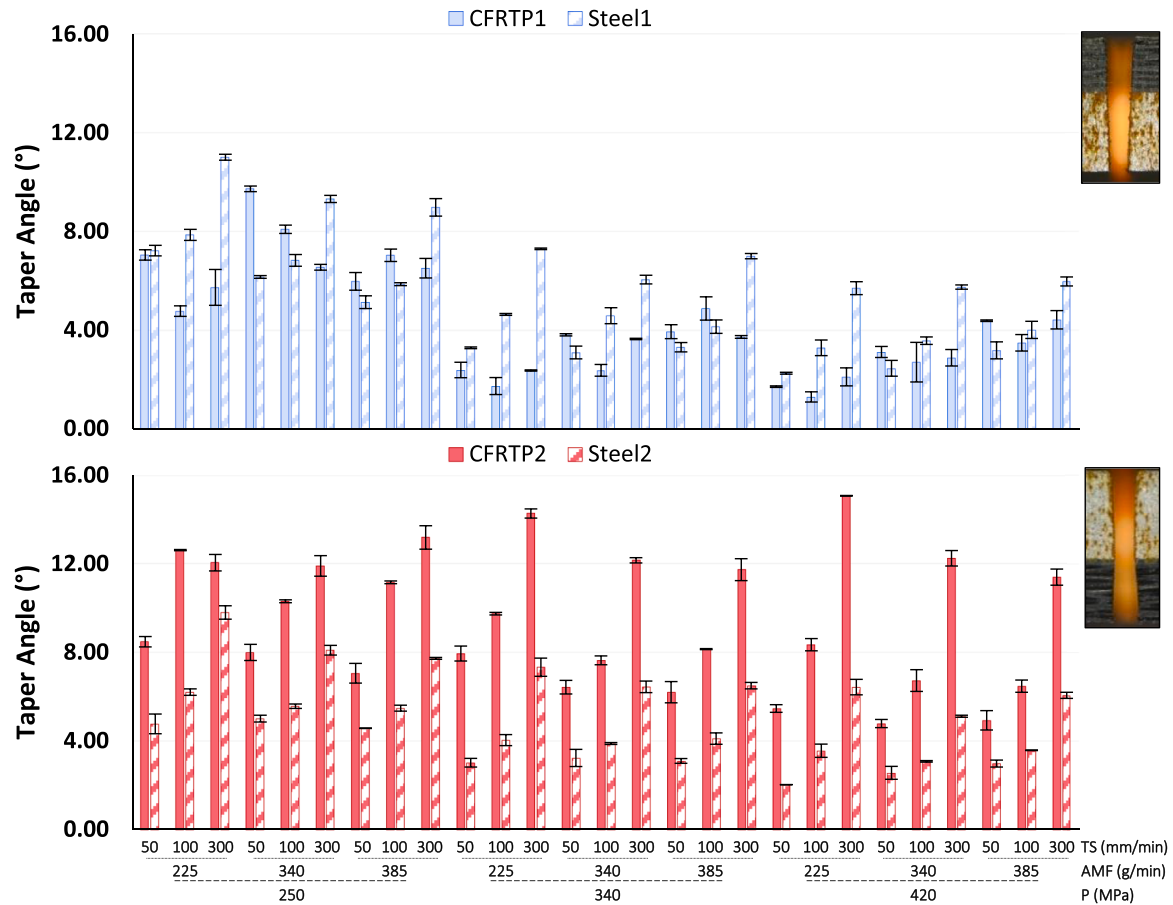


Fig. 21. Comparison between experimental and predicted taper values for both stacking configurations.

Table 4

ANOVA analysis of the taper angle for each material and stacking configuration.

Source	DF	Adj SS	Adj MS	F-Value	P-Value
<b>CFRT1</b>					
Model	9	107.073	11.8970	14.96	0.000
Pressure (MPa)	1	62.688	62.6882	78.80	0.000
Abrasive Mass Flow (g/min)	1	11.782	11.7818	14.81	0.001
Traverse Speed (mm/min)	1	0.996	0.9960	1.25	0.279
Error	17	13.524	0.7955		
Total	26	120.597			
<b>Steel1</b>					
Model	9	127.975	14.2195	174.95	0.000
Pressure (MPa)	1	58.742	58.7419	722.74	0.000
Abrasive Mass Flow (g/min)	1	1.5880	1.5875	19.53	0.000
Traverse Speed (mm/min)	1	53.600	53.5996	659.48	0.000
Error	17	1.382	0.0813		
Total	26	129.357			
<b>CFRT2</b>					
Model	9	220.829	24.5370	34.80	0.000
Pressure (MPa)	1	12.277	12.2770	17.42	0.001
Abrasive Mass Flow (g/min)	1	10.194	10.1940	14.46	0.001
Traverse Speed (mm/min)	1	165.985	165.985	235.44	0.000
Error	17	11.985	0.7050		
Total	26	232.814			
<b>Steel2</b>					
Model	9	94.369	10.4854	139.39	0.000
Pressure (MPa)	1	26.627	26.6279	353.99	0.000
Abrasive Mass Flow (g/min)	1	1.0346	1.0346	13.75	0.002
Traverse Speed (mm/min)	1	58.975	58.9756	784.02	0.000
Error	17	1.2788	0.0752		
Total	26	95.647			

and pressure, very close trends between  $R_a$  and  $R_z$  are observed for both case studies (Fig. 18 and Fig. 19). In addition, the relationship between composite material and steel is kept as the first material shows higher values.

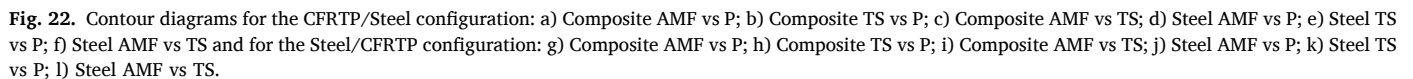
In a general way, an increase in traverse speed destabilizes the waterjet, especially for 300 mm/min, reducing its capacity to machine. This, together with the fact that two dissimilar materials have to be machined at the same time, produces a significant increase in  $R_a$  and  $R_z$  values in both stacking configurations. As with the taper obtained, to minimise this destabilisation and keep the machining capacity of the jet, the increase in hydraulic pressure allows the influence of speed on quality to be reduced by reducing the values. When the traverse speed is maximum (300 mm/min) the jet is unable to machine both materials in their totality at the same time interval which causes a delay between the upper and lower widths.

This causes a groove zone or "lag" in the final part of the material which increases the roughness in that region and increases the dispersion of results obtained in [63], especially on steel (Fig. 20).

### 3.3. Statistical analysis and contour diagrams in taper angle

In this section the statistical influence of the cutting parameters on the obtained conicity is explained. In addition, predictive models are developed, being of great interest for the industrial application. Predictive models of the surface quality have not been represented because the adjustments obtained are not suitable. A fundamental aspect in machining is that the product is within the specified tolerances at the macro-geometric (taper) and micro-geometric (surface quality) level. Nevertheless, due to the type of structure that has been machined and that the technology applied is orientated to the machining of flat





Thus, due to the turbulence of the waterjet in the interlayer of a hybrid structure and the influence of the stacking order in the machining of the same make the taper defect a key parameter to control and evaluate. In order to determine the most influential cutting parameters

In contrast, the results obtained in steel machining are similar in both

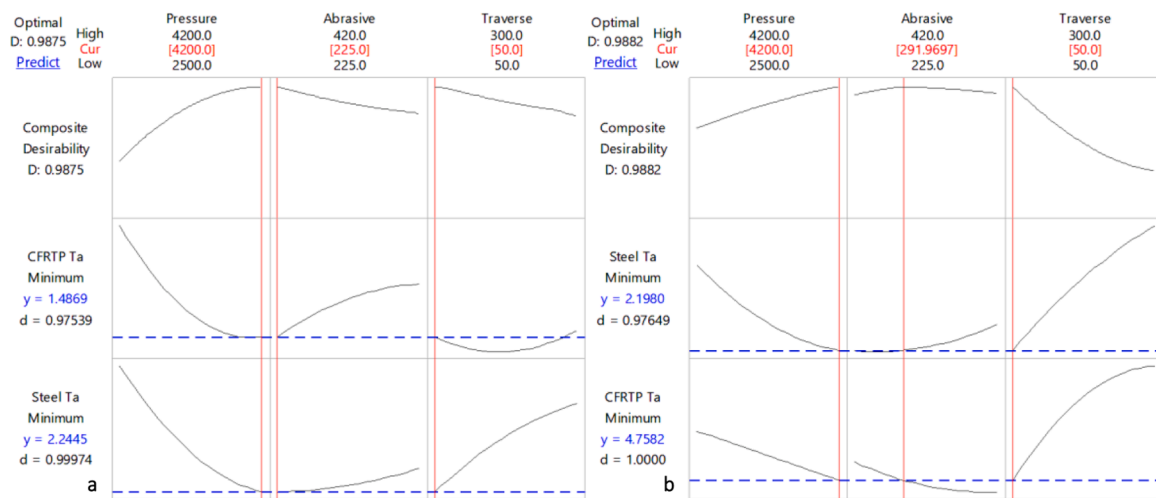


**Fig. 23.** Optimal combination of cutting parameters according to the predictive models obtained that minimize the taper after machining for: a) CFRT/Steel; b) Steel/CFRT.

configurations. However, for the CFRT/Steel configuration, hydraulic pressure is the most important parameter with a significance very close to the traverse speed. In contrast, when the stack is Steel/CFRT the hydraulic pressure is not so influential, the main parameter in machining being the waterjet traverse speed.

In turn, these results have been modelled by means of a second order polynomial equation, in order to obtain predictive models and their corresponding contour diagrams [64] in the Fig. 22.

Adjustments of 88.79% and 98.93% have been obtained for the composite material and steel respectively, in CFRT/Steel configuration. For the Steel/CFRT configuration, adjustments of 94.85% and 98.66% have been obtained. In general, reduced taper angle values are obtained by increasing the hydraulic pressure, setting values between 225 g/min and 340 g/min abrasive mass flow and reducing the traverse speed.

Based on the previous models, the lowest taper angles in both materials can be achieved when a combination of a pressure of 420 MPa, an abrasive mass flow of 291 g/min and a traverse speed of 50 mm/min are used for the Steel/CFRT configuration. In the case of CFRT/Steel, lower taper angles are given by the use of the same parameters, but reducing abrasive mass flow up to 225 g/min (Fig. 23). This figure shows in red the combination of cutting parameters that reduces the taper angle in both materials and stacking configurations based on the predictive models obtained. On the other hand, the dashed blue lines refer to the minimum value of the variable to be optimised (taper angle) obtained with the proposed combination of cutting parameters.

## Conclusions

Machining dissimilar materials in the form of hybrid structure is a current line of research of great interest. The difference in mechanical properties and their stacking order directly affects the final geometrical quality after abrasive water jet machining. This is due to the generation of a taper defect inherent to the process due to the loss of kinetic energy.

Traditional methodologies have evaluated this defect in a very general way by means of a ratio between widths. In this article, a more accurate methodology is proposed through image processing. This has made it possible to obtain maximum deviations of 0.45°.

A potential trend has been established between hydraulic pressure and taper angle obtained at 99% settings. In addition, second-order polynomial models with fits above 90% have been obtained.

The stacking order of the materials has been identified as a key factor in the final geometric quality. It directly affects the kinetic energy loss as a function of the machinability of both materials. This produces a

variation in the conical geometry of the structure.

The influence of the cutting parameters on the taper angle has been determined by means of an ANOVA analysis. Thus, hydraulic pressure is the most influential parameter in the CFRT/Steel configuration while in the Steel/CFRT configuration the most decisive parameter is the traverse speed. Pressures close to 420 MPa increase the kinetic energy of the water jet and its penetration capacity by minimizing the taper in both materials. On the other hand, traverse speed values close to 50 mm/min offer a greater stabilization of the water jet by minimizing the RCR zone and the ratio between the upper and lower width.

Consequently, the combination of a hydraulic pressure of 420 MPa, an abrasive mass flow of 225 g/min and a travel speed of 50 mm/min has been determined as the combination of cutting parameters that minimizes the conicity in both materials and stacking configurations.

Finally, the surface quality has been evaluated in terms of  $R_a$  and  $R_z$  and related to the cutting parameters. The influence of a high hydraulic pressure combined with a low traverse speed has been confirmed in order to keep the machining capacity of the jet and to generate a clean and low roughness surface. Furthermore, similar trends have been determined for  $R_a$  and  $R_z$ . Lag defects have been observed when the traverse speed is 300 mm/min. Moreover, due to the detachment of the thermoplastic matrix and the hydrodistortion defect, roughness values are always higher in the composite material.

## Author contributions

Developed machining tests: F.B.; Data treatment: F.B.; Bibliographic search: F.B.; Conclusions of the work: F.B. Analysis of the influence of parameters: F.B.; Writing the original manuscript and tables: F.B.; Figure elaboration: F.B. and A.S; Manuscript and grammar review: M.B., B.S. and J.S.; Critical comments on the final manuscript: A.S., M.B., B.S. and J.S. The authors read and approved the final manuscript.

## Funding

This work has been developed under the support of a pre-doctoral industrial fellow financed by NANOTURES SL, the Mechanical Engineering and Industrial Design department and the Vice-Rector's Office for Scientific Policy of the University of Cadiz.

## Declaration of Competing Interest

The authors declare no conflict of interest.

## References

- [1] Jiao J, Xia S, Xu Z, Ye Y, Sheng L, Zhang W. Laser direct joining of CFRTP and aluminium alloy with a hybrid surface pre-treating method. *Compos Part B Eng* 2019;173:106911. <https://doi.org/10.1016/j.compositesb.2019.106911>.
- [2] Berger S, Schmidt M. Laser transmission welding of CFRTP using filler material. *Phys Procedia* 2014;56:1182–90. <https://doi.org/10.1016/j.phpro.2014.08.033>.
- [3] Goto K, Imai K, Arai M, Ishikawa T. Shear and tensile joint strengths of carbon fiber-reinforced thermoplastics using ultrasonic welding. *Compos Part A Appl Sci Manuf* 2019;116:126–37. <https://doi.org/10.1016/j.compositesa.2018.10.032>.
- [4] Ishikawa T, Amaoka K, Masubuchi Y, Yamamoto T, Yamanaka A, Arai M, et al. Overview of automotive structural composites technology developments in Japan. *Compos Sci Technol* 2018;155:221–46. <https://doi.org/10.1016/j.compscitech.2017.09.015>.
- [5] Bernd-Arno B, Sven H, Nenad G, Moritz M-C, Tim W, André N. Forming and Joining of Carbon-Fiber-Reinforced Thermoplastics and Sheet Metal in One Step. *Procedia Eng* 2017;183:227–32. <https://doi.org/10.1016/j.proeng.2017.04.026>.
- [6] Arhant M, Davies P. Thermoplastic matrix composites for marine applications. *Mar. Compos., Elsevier* 2019:31–53. <https://doi.org/10.1016/B978-0-08-102264-1.00002-9>.
- [7] Jiao J, Xu Z, Wang Q, Sheng L, Zhang W. CFRTP and stainless steel laser joining: thermal defects analysis and joining parameters optimization. *Opt Laser Technol* 2018;103:170–6. <https://doi.org/10.1016/j.optlastec.2018.01.023>.
- [8] Pahuja R, M. R. Abrasive water jet machining of Titanium (Ti6Al4V)–CFRP stacks – a semi-analytical modeling approach in the prediction of kerf geometry. *J Manuf Process* 2019;39:327–37. <https://doi.org/10.1016/j.jmapro.2019.01.041>.
- [9] Mahdi A, Turki Y, Habak M, Salem M, Bouaziz Z. Experimental study of thrust force and surface quality when drilling hybrid stacks. *Int J Adv Manuf Technol* 2020;107:3981–94. <https://doi.org/10.1007/s00170-020-05252-7>.
- [10] Xu J, Zhou L, Chen M, Ren F. Experimental study on mechanical drilling of carbon/epoxy composite-Ti6Al4V stacks. *Mater Manuf Process* 2019;34:715–25. <https://doi.org/10.1080/10426914.2019.1594275>.
- [11] Fernandez-Vidal S, Fernandez-Vidal S, Batista M, Salguero J. Tool wear mechanism in cutting of stack CFRP/UNS A97075. *Materials (Basel)* 2018;11:1276. <https://doi.org/10.3390/ma11081276>.
- [12] Santhanakrishnan Balakrishnan V, Obrosova A, Kuke F, Seidlitz H, Weiß S. Influence of metal surface preparation on the flexural strength and impact damage behaviour of thermoplastic FRP reinforced metal laminate made by press forming. *Compos Part B Eng* 2019;173:106883. <https://doi.org/10.1016/j.compositesb.2019.05.094>.
- [13] Adesta EYT, Riza M, Avicena. Comparative investigation on tool wear during end milling of AISI H13 steel with different tool path strategies. *IOP Conf. Ser. Mater. Sci. Eng.* 2018;343:012020. <https://doi.org/10.1088/1757-899X/343/1/012020>. IOP Publishing.
- [14] Rosnan R, Murad MN, Azmi AI, Shyha I. Effects of minimal quantity lubricants reinforced with nano-particles on the performance of carbide drills for drilling nickel-titanium alloys. *Tribol Int* 2019;136:58–66. <https://doi.org/10.1016/j.triboint.2019.03.029>.
- [15] Dionne J, Sorbo NW. Benefits of CO<sub>2</sub> cooling as a cooling technology for drilling of stackup composite structures. *CAMX 2015 - Compos. Adv. Mater. Expo 2015*: 890–905.
- [16] Impero F, Dix M, Squillace A, Prisco U, Palumbo B, Tagliaferri F. A comparison between wet and cryogenic drilling of CFRP/Ti stacks. *Mater Manuf Process* 2018;33:1354–60. <https://doi.org/10.1080/10426914.2018.1453162>.
- [17] Ghani JA, Rizal M, Che Haron CH. Performance of green machining: a comparative study of turning ductile cast iron FCD700. *J Clean Prod* 2014;85:289–92. <https://doi.org/10.1016/j.jclepro.2014.02.029>.
- [18] Klocke F, Eisenblätter G. Dry cutting - state of research. *VDI Berichte* 1998;46: 159–88. [https://doi.org/10.1016/S0007-8506\(07\)60877-4](https://doi.org/10.1016/S0007-8506(07)60877-4).
- [19] Khanna N, Agrawal C, Gupta MK, Song Q, Singla AK. Sustainability and machinability improvement of nimonicon-90 using indigenously developed green hybrid machining technology. *J Clean Prod* 2020;121402. <https://doi.org/10.1016/j.jclepro.2020.121402> (In press).
- [20] Wang X, Kwon PY, Sturtevant C, Kim DDW, Lantrip J. Comparative tool wear study based on drilling experiments on CFRP/Ti stack and its individual layers. *Wear* 2014;317:265–76. <https://doi.org/10.1016/j.wear.2014.05.007>.
- [21] Erturk AT, Vatansver F, Yazar E, Guven EA, Sinmazcelik T. Effects of cutting temperature and process optimization in drilling of GFRP composites. *J Compos Mater* 2020. <https://doi.org/10.1177/0021998320947143>.
- [22] Masek P, Zeman P, Kolar P. Edge trimming of C /PPS plates. *Int J Adv Manuf Technol* 2018;101:157–70. <https://doi.org/10.1007/s00170-018-2857-1>.
- [23] El-Hofy M, Helmy MO, Escobar-Palaflox G, Kerrigan K, Scaife R, El-Hofy H. Abrasive water jet machining of multidirectional CFRP laminates. *Procedia CIRP* 2018;68:535–40. <https://doi.org/10.1016/j.procir.2017.12.109>.
- [24] Vu NP, Le XH, Nguyen DN, Luu AT, Nguyen TT, Tran NG, et al. Optimizing replaced nozzle diameter of abrasive blasting systems using experiment technique design. *Appl Sci* 2020;10. <https://doi.org/10.3390/app10113920>.
- [25] Perec A. Environmental aspects of abrasive water jet cutting. *Rocz Ochr Sr* 2018;20:258–74.
- [26] Hlaváč LM, Bańkowski D, Krajcarz D, Štefek A, Tyč M, Młynarczyk P. Abrasive waterjet (AWJ) forces—indicator of cutting system malfunction. *Materials (Basel)* 2021;14:1683. <https://doi.org/10.3390/ma14071683>.
- [27] Melentiev R, Fang F. Recent advances and challenges of abrasive jet machining. *CIRP J Manuf Sci Technol* 2018. <https://doi.org/10.1016/j.cirpj.2018.06.001>.
- [28] Li M, Huang M, Chen Y, Gong P, Yang X. Effects of processing parameters on kerf characteristics and surface integrity following abrasive waterjet slotting of Ti6Al4V/CFRP stacks. *J Manuf Process* 2019;42:82–95. <https://doi.org/10.1016/j.jmapro.2019.04.024>.
- [29] Li M, Lin X, Yang X, Wu H, Meng X. Study on kerf characteristics and surface integrity based on physical energy model during abrasive waterjet cutting of thick CFRP laminates. *Int J Adv Manuf Technol* 2021;113:73–85. <https://doi.org/10.1007/s00170-021-06590-w>.
- [30] Mayuet PF, Girot F, Lamkiz A, Fernández-Vidal SR, Salguero J, Marcos M. SOM/SEM based characterization of internal delaminations of CFRP samples machined by AWJM. *Procedia Eng* 2015;132:693–700. <https://doi.org/10.1016/j.proeng.2015.12.549>.
- [31] Bañón F, Sambruno A, González-Rovira L, Vazquez-Martinez JM, Salguero J. A review on the abrasive water-jet machining of metal–carbon fiber hybrid materials. *Metals (Basel)* 2021;11:29. <https://doi.org/10.3390/met11010164>.
- [32] Bañón F, Simonet B, Sambruno A, Batista M, Salguero J. On the surface quality of CFRTP/steel hybrid structures machined by AWJM. *Metals (Basel)* 2020;10:983. <https://doi.org/10.3390/met10070983>.
- [33] Ruiz-García R, Mayuet Ares P, Vazquez-Martinez J, Salguero Gómez J. Influence of abrasive waterjet parameters on the cutting and drilling of CFRP/UNS A97075 and UNS A97075/CFRP stacks. *Materials (Basel)* 2018;12:107. <https://doi.org/10.3390/ma12010107>.
- [34] Pahuja R, Ramulu M, Hashish M. Surface quality and kerf width prediction in abrasive water jet machining of metal-composite stacks. *Compos Part B Eng* 2019;175:107134. <https://doi.org/10.1016/j.compositesb.2019.107134>.
- [35] Rajesh M, Rajkumar K, Annamalai VE. Abrasive water jet machining on Ti metal-interleaved basalt-flax fiber laminate. *Mater Manuf Process* 2021;36:329–40. <https://doi.org/10.1080/10426914.2020.1832692>.
- [36] Pahuja R, Ramulu M, Hashish M. Abrasive waterjet profile cutting of thick titanium/graphite fiber metal laminate. *Proc ASME 2016 Int Mech Eng Congr Expo IMECE2016* 2016:1–11. <https://doi.org/10.1115/IMECE201667136>.
- [37] Kechagias J, Petropoulos G, Vaxevanidis N. Application of Taguchi design for quality characterization of abrasive water jet machining of TRIP sheet steels. *Int J Adv Manuf Technol* 2012;62:635–43. <https://doi.org/10.1007/s00170-011-3815-3>.
- [38] Yang X, Lin X, Li M, Jiang X. Experimental study on surface integrity and kerf characteristics during abrasive waterjet and hybrid machining of CFRP laminates. *Int J Precis Eng Manuf* 2020;21:2209–21. <https://doi.org/10.1007/s12541-020-00415-8>.
- [39] Bañón F, Sambruno A, Batista M, Simonet B, Salguero J. Study of the surface quality of carbon fiber–reinforced thermoplastic matrix composite (CFRTP) machined by abrasive water jet (AWJM). *Int J Adv Manuf Technol* 2020;107: 3299–313. <https://doi.org/10.1007/s00170-020-05215-y>.
- [40] Alberdi A, Artaza T, Suárez A, Rivero A, Girot F. An experimental study on abrasive waterjet cutting of CFRP/Ti6Al4V stacks for drilling operations. *Int J Adv Manuf Technol* 2016;86:691–704. <https://doi.org/10.1007/s00170-015-8192-x>.
- [41] Zhang S, Ji L, Wu Y, Chen M, Zhou W. Exploring a new method to obtain the 3D abrasive water jet profile. *Int J Adv Manuf Technol* 2020:4797–809. <https://doi.org/10.1007/s00170-020-05185-1>.
- [42] Manoj KR, Shet M, Naveen V, Murthy S, Srinivas S. Kerf Analysis and delamination study on fiber reinforced composites cut by abrasive water jet. *Mater Today Proc* 2021. <https://doi.org/10.1016/j.matpr.2020.10.408>.
- [43] Singh D, Shukla RS. Investigation of kerf characteristics in abrasive water jet machining of inconel 600 using response surface methodology. *Def Sci J* 2020;70: 313–22. <https://doi.org/10.14429/dsj.70.14323>.
- [44] Youssef HA, El-Hofy HA, Abdelaziz AM, El-Hofy MH. Accuracy and surface quality of abrasive waterjet machined CFRP composites. *J Compos Mater* 2020. <https://doi.org/10.1177/0021998320974428>.
- [45] Llanto JM, Tolouei-Rad M, Vafadar A, Aamir M. Recent progress trend on abrasive waterjet cutting of metallic materials: a review. *Appl Sci* 2021;11:3344. <https://doi.org/10.3390/app11083344>.
- [46] Thakur RK, Singh KK. Abrasive waterjet machining of fiber-reinforced composites: a state-of-the-art review. *J Brazilian Soc Mech Sci Eng* 2020;42. <https://doi.org/10.1007/s40430-020-02463-7>.
- [47] Perumal A, Kailasanathan C, Wilson VH, Sampath Kumar T, Stalin B, Rajkumar PR. Machinability of titanium alloy 6242 by AWJM through Taguchi method. *Mater Today Proc* 2021. <https://doi.org/10.1016/j.matpr.2021.04.067>.
- [48] Karmiris-Obratański P, Karkalos NE, Kudelski R, Papazoglou EL, Markopoulos AP. On the effect of multiple passes on kerf characteristics and efficiency of abrasive waterjet cutting. *Metals (Basel)* 2021;11:1–14. <https://doi.org/10.3390/met11010074>.
- [49] Mamalis D, Obando W, Koutsos V, Blackford JR, Ó Brádaigh CM, Ray D. Novel thermoplastic fibre-metal laminates manufactured by vacuum resin infusion: the effect of surface treatments on interfacial bonding. *Mater Des* 2019;162:331–44. <https://doi.org/10.1016/j.matdes.2018.11.048>.
- [50] Sheng LY, Wang FY, Wang Q, Jiao JK. Shear strength optimization of laser-joined polyphenylene sulfide-based CFRTP and stainless steel. *Strength Mater* 2018;50: 824–31. <https://doi.org/10.1007/s11223-018-0028-0>.
- [51] Martinsen K, Hu SJ, Carlson BE. Joining of dissimilar materials. *CIRP Ann* 2015;64: 679–99. <https://doi.org/10.1016/j.cirp.2015.05.006>.
- [52] Linghoff D, Haghani R, Al-Emrani M. Carbon-fibre composites for strengthening steel structures. *Thin-Walled Struct* 2009;47:1048–58. <https://doi.org/10.1016/j.tws.2008.10.019>.
- [53] Bañón F, Sambruno A, Batista M, Simonet B, Salguero J. Surface quality and free energy evaluation of s275 steel by shot blasting, abrasive water jet texturing and laser surface texturing. *Metals (Basel)* 2020;10:290. <https://doi.org/10.3390/met10020290>.

- [54] Sambruno A, Bañon F, Salguero J, Simonet B, Batista M. Kerf taper defect minimization based on abrasive waterjet machining of low thickness thermoplastic carbon fiber composites C/TPU. *Materials (Basel)* 2019;12:4192. <https://doi.org/10.3390/ma12244192>.
- [55] Kumar S, Laxminarayana P, Ashok Kumar U. Optimization of process parameters on kerf width & taper angle on en-8 carbon steel by abrasive water jet machining. 3rd Natl. Conf. Recent Trends Innov. Mech. Eng., Hyderabad, India 2019:281–7.
- [56] Manoj M, Jinu GR, Muthuramalingam T. Multi response optimization of AWJM process parameters on machining TiB2 particles reinforced Al7075 composite using Taguchi-DEAR methodology. *Silicon* 2018;10:2287–93. <https://doi.org/10.1007/s12633-018-9763-x>.
- [57] Dhanawade A, Kumar S. Experimental study of delamination and kerf geometry of carbon epoxy composite machined by abrasive water jet. *J Compos Mater* 2017;51:3373–90. <https://doi.org/10.1177/0021998316688950>.
- [58] Mayuet Ares PF, Rodríguez-Parada L, Gómez-Parra A, Batista M. Characterization and defect analysis of machined regions in Al-SiC metal matrix composites using an abrasive water jet machining process. *Appl Sci* 2020;10:1512.
- [59] Kakinuma Y, Ishida T, Koike R, Klemme H, Denkena B, Aoyama T. Ultrafast feed drilling of carbon fiber-reinforced thermoplastics. *Procedia CIRP* 2015;35:91–5. <https://doi.org/10.1016/j.procir.2015.08.074>.
- [60] Ming Ming IW, Azmi AI, Chuan LC, Mansor AF. Experimental study and empirical analyses of abrasive waterjet machining for hybrid carbon/glass fiber-reinforced composites for improved surface quality. *Int J Adv Manuf Technol* 2017;1–14. <https://doi.org/10.1007/s00170-017-1465-9>.
- [61] Selvan CP, Midhunchakkaravarthy D, Pillai SR, Madara SR. Investigation on abrasive waterjet machining conditions of mild steel using artificial neural network. *Mater Today Proc* 2019;19:233–9. <https://doi.org/10.1016/j.matpr.2019.06.757>.
- [62] A. Dumbhare P, Dubey S, V. Deshpande Y, Andhare AB, Barve PS. Modelling and multi-objective optimization of surface roughness and kerf taper angle in abrasive water jet machining of steel. *J Brazilian Soc Mech Sci Eng* 2018;40:259. <https://doi.org/10.1007/s40430-018-1186-5>.
- [63] Chithirai M, Selvan P, Mohana N, Raju S. Assessment of process parameters in abrasive waterjet cutting of stainless steel. *Int J Adv Eng Technol* 2011;1:2231–1963.
- [64] Jagadish Bhowmik S, Ray A. Prediction and optimization of process parameters of green composites in AWJM process using response surface methodology. *Int J Adv Manuf Technol* 2016;87:1359–70. <https://doi.org/10.1007/s00170-015-8281-x>.